Molecular Therapy
Original Article

Overcoming Limitations Inherent in Sulfamidase to Improve Mucopolysaccharidosis IIIA Gene Therapy

Yonghong Chen,[1] Shujuan Zheng,[1] Luis Tecedor,[1] and Beverly L. Davidson[1,2]

[1]Raymond G. Perelman Center for Cellular and Molecular Therapeutics, The Children's Hospital of Philadelphia, Philadelphia, PA 19104, USA; [2]Department of Pathology and Laboratory Medicine, University of Pennsylvania, Philadelphia, PA 19104, USA

Sulfamidase (SGSH) deficiency causes mucopolysaccharidosis type IIIA (MPS IIIA), a lysosomal storage disease (LSD) that affects the CNS. In earlier work in LSD mice and dog models, we exploited the utility of adeno-associated viruses (AAVs) to transduce brain ventricular lining cells (ependyma) for secretion of lysosomal hydrolases into the cerebrospinal fluid (CSF), with subsequent distribution of enzyme throughout the brain resulting in improved cognition and extending lifespan. A critical feature of this approach is efficient secretion of the expressed enzyme from transduced cells, for delivery by CSF to nontransduced cells. Surprisingly, we found that SGSH was poorly secreted from cells, resulting in retention of the expressed product. Using site-directed mutagenesis of native SGSH, we identified an improved secretion variant that also displayed enhanced uptake properties that were mannose-6-phosphate receptor independent. In studies in MPS IIIA-deficient mice, ependymal transduction with AAVs expressing variant SGSH improved spatial learning and reduced memory deficits, substrate accumulation, and astrogliosis. Secondary lysosomal enzyme elevations in the CSF and brain parenchyma were also resolved. In contrast, ependymal transduction with AAVs expressing wild-type SGSH had significantly lower CSF SGSH levels and limited impacts on behavior. These results demonstrate the utility of a previously undescribed SGSH variant for improved MPS IIIA brain gene therapy.

INTRODUCTION

Mucopolysaccharidosis type IIIA (MPS IIIA) is a lysosomal storage disease (LSD) caused by sulfamidase (SGSH) deficiency due to mutations in *SGSH*. MPS IIIA is characterized by progressive neurodegeneration accompanied by loss of social skills and aggressive behavior, hyperactivity, and sleep disturbance. Somatic features are often mild and variable.[1]

Therapies advanced for MPS IIIA can essentially be classified as enzyme replacement therapy (ERT), either through infusion of the recombinant protein or by gene-therapy-based methods. In early work, infusion of purified SGSH intravenously at birth,[2] or into the cerebrospinal fluid (CSF) in adult mice models of MPS IIIA,[3] improved behavior and neuropathology. More recently, using a canine model of MPS IIIA, infusion of purified SGSH into the CSF into intrathecal, intracisternal, or intraventricular spaces significantly reduced primary and secondary substrate levels in brain. However, only ERT delivery via the ventricles ameliorated microgliosis in the deep cerebral cortex.[4] These advances led to a clinical trial to evaluate SGSH delivery to MPS IIIA patients (clinical trial NCT01299727), which was completed in 2016.

ERT via gene therapy takes advantage of a vector's ability to deliver an expression cassette resulting in SGSH production in transduced cells, presumably for the life of that cell or at least for many years. Unlike ERT by protein infusion, gene-therapy-based methods require viral uptake in target cells, expression in transduced cells, secretion of the proenzyme, and subsequent uptake, lysosomal delivery, and finally processing to the active enzyme in non-transduced cells. In some cases, the non-transduced cells reside far from the population of cells that were transduced. For MPS IIIA, recent work in mice models has shown robust improvements after CSF infusion[5] or systemic administration[6,7] of recombinant adeno-associated viruses (rAAVs) expressing SGSH, resulting in increased SGSH activity throughout the brain and peripheral organs, normalization of behavioral deficits, and prolonged survival.

The first clinical trial of gene therapy for MPS IIIA treatment was performed with serotype rh.10AAV vector encoding a *SGSH* transgene, delivered by multiple intracerebral injections into the brain parenchyma. Although tolerated, clinical improvement of patients was moderate.[8] The inconsistency with results obtained in MPS IIIA mice and dog studies may simply be because of size differences between mice, dog, and human brain, or other factors. Interestingly, viral uptake can be impacted by disease in LSD mice, likely because of changes in extracellular matrix components that can occur in the setting of altered degradative pathways.[9,10] Additionally, the success

Received 7 September 2017; accepted 12 January 2018;
https://doi.org/10.1016/j.ymthe.2018.01.010.

Correspondence: Beverly L. Davidson, The Children's Hospital of Philadelphia, 5060 CTRB, 3501 Civic Center Boulevard, Philadelphia, PA 19104, USA.
E-mail: davidsonbl@email.chop.edu

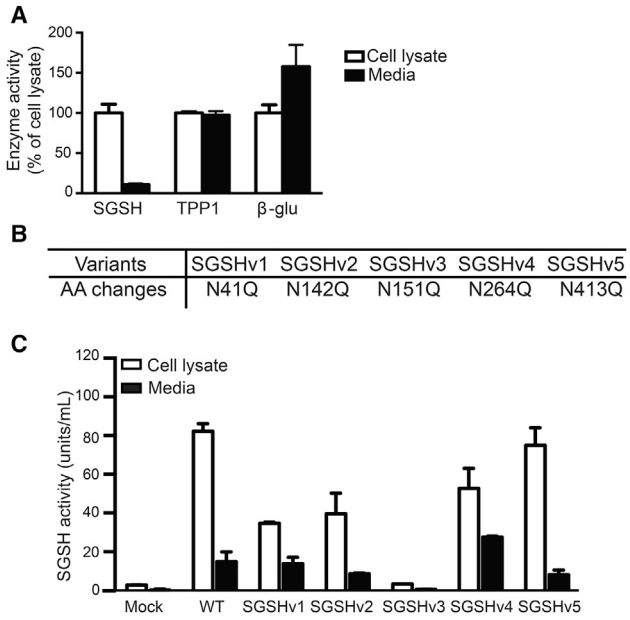

Figure 1. Comparison of the Secretory Properties of Various Lysosomal Enzymes *In Vitro* and the Effects of Abrogating M6P Sites on SGSH Secretion and Activity

(A) HEK293 cells were transfected with plasmids expressing SGSH, TPP1, or β-glu. After 72 hr, cells and media were harvested and enzyme activities assessed by enzyme activity assay; n = 3 biological replicates, in triplicate. Data represent mean ± SD. (B) Five SGSH variants were generated by site-directed mutagenesis to introduce N-to-Q mutations at N-glycosylation sites at amino acids (aa) 41, 142, 151, 264, and 413 as indicated. (C) Activity levels of WT or variant SGSH after transfection of expression vectors into HEK293 cells. Cells and media were collected and assayed for SGSH enzyme activity 72 hr after transfection; n = 3 biological replicates, in triplicate. Data represent mean ± SD.

of cross-correction relies on effective secretion from transduced cells and distribution to non-transduced cells.

The methods described above use gene-corrected neurons and glia distributed throughout the CNS as a source of recombinant protein, following intraparenchymal, intraventricular, or intravascular administration. An example of the latter is the intravascular administration of AAV9 expressing SGHS (clinical trial NCT02716246). Another method to achieve widespread distribution of recombinant protein throughout the CNS is to co-opt CSF flow. Indeed, earlier work showed that ERT to the CSF or gene transfer to the ependyma cells lining the ventricles could protect or reverse CNS deficits in mice and dog models of LSD.[11–13] Currently, it is unknown whether the properties of lysosomal hydrolases with robust secretion following expression from transduced cells, such as β-glucuronidase (β-glu) or tripeptidyl peptidase (TPP1), are reflective of the bulk of lysosomal enzymes.

As a first step to translate our earlier work showing the effectiveness of ependyma as a useful target for LSD gene therapies in models of β-glu deficiency (MPS VII)[13] and TPP1 deficiency,[12] a form of Batten disease[14] to MPS IIIA, we compared the ability of the respective recombinant proteins to be secreted from cells. Surprisingly, we found that SGSH was poorly secreted from cells, with most of the product retained in the cytoplasm. Here, we tested the hypothesis that variants of SGSH with improved secretory properties could be generated, and that they would be therapeutically superior to the wild-type enzyme when tested in the setting of MPS IIIA deficiency.

RESULTS

Altering the Glycosylation of SGSH Improves Secretion

We first compared the secretory potential of SGSH with TPP1 and β-glu. HEK293 cells were transfected with identical expression plasmids except for the recombinant protein coding sequence. After 72 hr, the lysosomal enzyme activity in collected media and cell lysates was analyzed. As shown in Figure 1A, less than 20% of SGSH activity was detected in media compared with the cell lysate, while in TPP1- or β-glu-expressing cells, roughly 50%–60% was secreted, respectively.

Posttranslational modification of mannose or mannose 6-phosphate (M6P) on lysosomal enzymes occurs at N-linked oligosaccharide side chains. SGSH has five potential N-glycosylation consensus sequences (Asn-Xaa-Ser/Thr), with the glycan-accepting Asn residue at amino acid positions of 41, 142, 151, 264, and 413. Five SGSH enzyme variants were constructed with sequentially substituted Asn to Gln residues (Figure 1B; Table S1), and their secretory and uptake properties were evaluated.

SGSHv1-3 lowered the levels of activity in the media and cell lysates, with SGSHv3 abrogating nearly all activity (Figure 1C). In contrast, SGSH variant 4 (SGSHv4) showed greater levels of SGSH activity in media with lower levels of SGSH activity retained in cells, ∼60% that of wild-type transfected cells. These data suggest that SGSHv4 improves secretion and at the same time reduces the overload of additional SGSH within transfected cells (Figure 1C).

To monitor enzyme secretion temporally, we transfected HEK293 cells with plasmids expressing wild-type or SGSHv4, and enzyme activity and protein levels in media and cell lysates were monitored 24, 48, and 72 hr later. Cells transfected with SGSHv4 variant-expressing plasmids secreted SGSH more efficiently than those transfected with plasmids expressing the wild-type enzyme at all times. By 24 hr there were nearly four times more enzymes in the media of SGSHv4-transfected cells compared with cells transfected with wild-type SGSH expression vectors (Figure 2A). Conversely, cellular levels of SGSH activity were lower for SGSHv4- versus wild-type SGSH-expressing cells at all time points (Figure 2B). Western blots of cell lysates showed reduced levels of mature SGSHv4 in SGSHv4-expressing cells as well (Figures 2C and 2D), supporting the notion that more of the enzyme is secreted versus retained and processed into mature enzyme. The lower apparent molecular weight of SGSHv4 by western blot assay in both precursor and mature forms is presumably due to

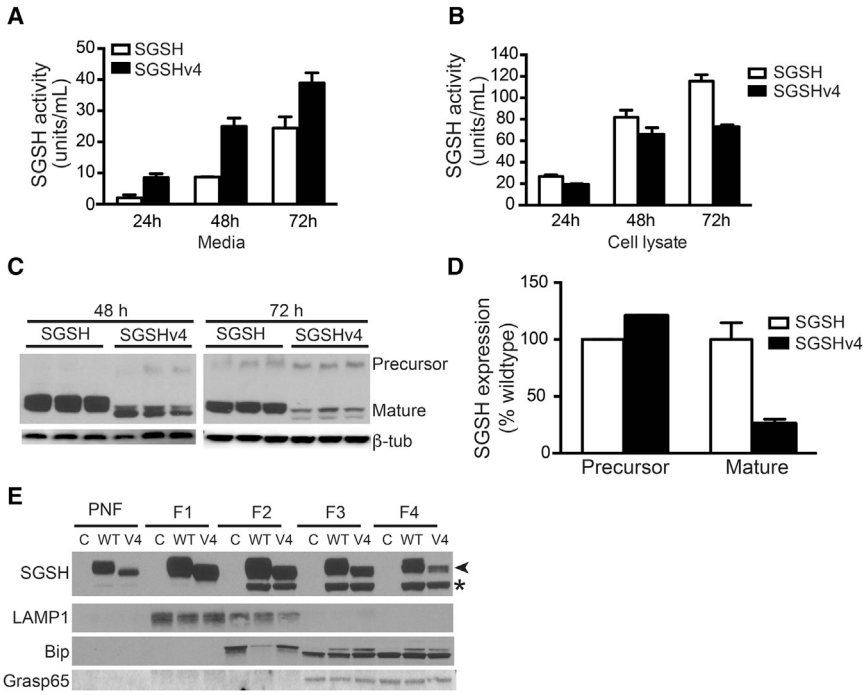

Figure 2. Temporal Analysis of WT SGSH and SGSHv4 Activity

HEK293 cells were transfected with vectors expressing WT SGSH or SGSHv4, the (A) media and (B and C) cells harvested at the indicated time points, and SGSH activity (A and B) or protein levels (C) assessed; n = 3 biological replicates, in triplicate. Data represent mean ± SD. (D) The ratio of WT SGSH to SGSHv4 protein levels in the cell lysate as assessed by western blot. Both precursor and mature forms were evaluated; n = 3 biological replicates. Data represent mean ± SD. (E) Representative western blot (of four biological replicates) indicating SGSH and SGSHv4 protein levels in the indicated fractions isolated after gradient centrifugation. LAMP1, Bip, and Grasp 65 were used to identify enrichment of lysosomal, ER, and Golgi markers, respectively. Asterisk (*) indicates unglycosylated SGSH; arrowhead indicates glycosylated SGSH. PNF, post-nuclear fraction.

the lower levels of phosphorylation as a result of the loss of the M6P site.

To further analyze intracellular trafficking, we assessed the SGSH and SGSHv4 levels in cells 72 hr after transfection by gradient fractionation and western blot analysis. The data show similar levels of unglycosylated SGSH and SGSHv4 in the Golgi and endoplasmic reticulum (ER) (Figure 2E, fractions 3 and 4), and less glycosylated SGSHv4 relative to the wild-type (WT) protein in these same fractions. This difference is also apparent in the total post-nuclear fraction, which represents the total intracellular fraction minus the nuclear pellet (Figure 2E, PNF). Together with data in Figures 2A–2D, there are diminished levels of glycosylated SGSHv4 relative to SGSH. This likely reflects increased secretion, rather than increased degradation.

In addition to M6P binding sites, we also explored SGSH ubiquitination sites. The rationale is that disturbance in ubiquitin-proteasome degradation will increase enzyme levels within cells and further improve secretion. In SGSH, 3 of 12 potential ubiquitination sites are active as evidenced by a proteome-wide *in vivo* ubiquitination study.[15] These sites (K103, K303, and K425) were sequentially modified by Arg substitution (Table S1). All modifications were neutral with regard to their impact on enzyme activity and had no impact on secretion (Figure S1). The ubiquitination variants were dropped from further evaluation.

As a third method to increase SGSH secretion, different signal peptides were tested. Three signal peptides from highly secretory lysosomal enzymes, iduronate-2-sulphatase, β-glu, and TPP1, were engineered to replace the SGSH signal peptide. Only iduronate-2-sulphatase and TPP1 signal peptides slightly increased (around 30%) secretion, whereas the β-glu signal peptide decreased SGSH levels in cell lysates and media (Figure S2A). Of note, signal peptide replacement with those from iduronate-2-sulphatase and TPP1 did not affect SGSH levels in cell lysates (Figure S2B). Given these modest results, we focused on SGSHv4 for further study.

SGSHv4 Uptake Is More Efficient and Is M6PR Independent

The underlying principal for cross-correction by gene therapy requires that the enzyme is effectively secreted from overexpressing (transduced) cells, and also that the secreted enzyme can be endocytosed by nontransduced cells. As such, we analyzed the uptake of WT and SGSHv4 in MPS IIIA patient fibroblasts. Conditioned media from HEK293 cells expressing WT SGSH or SGSHv4, normalized for equivalent SGSH activity, were applied to patient fibroblasts for 6 hr; then cells were collected and activity in cell lysates evaluated. To our surprise, the SGSHv4-expressed product was more efficiently taken up by patient fibroblasts compared with the WT enzyme, with >60% of the input of SGSHv4 entering the cells versus <40% for the WT enzyme (Figure 3A). Moreover, in the presence of 10 mM M6P, uptake of WT SGSH was blocked, but not SGSHv4 (Figure 3A). We next applied equivalent levels of enzyme harvested from conditioned media from cells transfected with plasmids expressing SGSH, SGSHv4, or from untransfected cells (control). The conditioned media were applied to MPS IIIA patient fibroblasts, removed 6 hr later, and cells fixed and imaged for visualization of internalized SGSH or SGSHv4. The expectant punctuate staining pattern was evident for both SGSH and SGSHv4, with the latter much more robust (Figure 3B). Cells from these experiments were also harvested prior to fixation and lysed for evaluation of protein levels by western blot. Both WT and SGSHv4 were processed to the mature enzyme once internalized, supporting lysosomal delivery (Figure 3C).

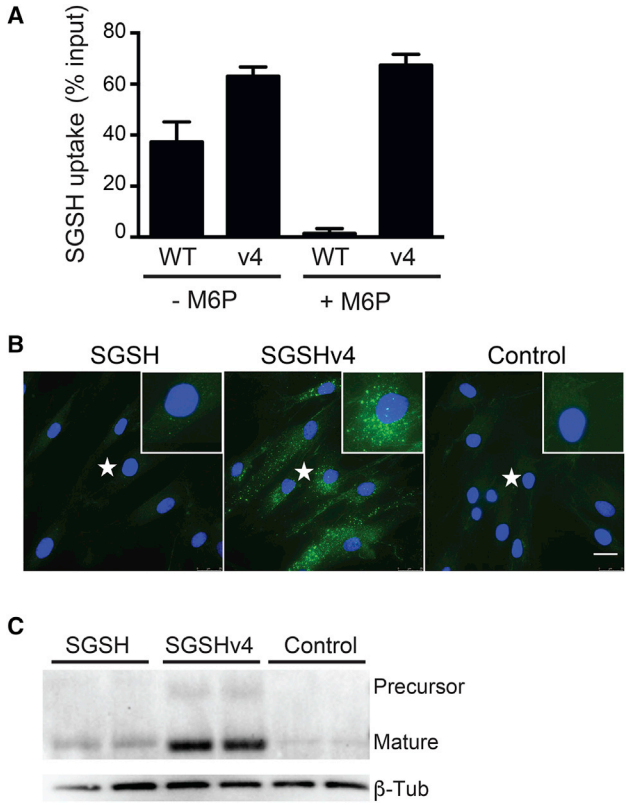

Figure 3. SGSH Uptake by MPS IIIA Patient Fibroblasts

(A) Conditioned media containing either WT SGSH or SGSHv4, plus or minus M6P, were applied to MPS IIIA patient fibroblasts and enzyme activity in cell lysates assessed 6 hr later. Data represent mean ± SD. (B) Immunohistochemistry for human SGSH after application of conditioned media to MPS IIIA fibroblasts. Conditioned media as in (A) was applied for 6 hr, after which the cells were fixed, stained for human SGSH, and imaged. Insets are enlargements of sites marked with an asterisk (*). Scale bar, 25 μm. (C) Conditioned media containing SGSH or SGSHv4 were applied to MPS IIIA patient fibroblasts for 6 hr, and SGSH protein levels in cell lysates were analyzed by western blot. For all panels, n = 3 biological replicates, in triplicate.

AAV.SGSHv4 Has Improved Therapeutic Properties *In Vivo*

To compare SGSHv4 with SGSH *in vivo*, we injected MPS IIIA model mice intraventricularly with AAV4 vectors encoding the different transgenes (AAV.SGSH or AAV.SGSHv4) at the same dose; AAV4 in mice targets ependymal cells exclusively.[13,16] Mice were tested using the Morris water maze 12 weeks following gene transfer. In AAV.SGSHv4-treated MPS IIIA mice, the latency to find the platform on day 5 was equivalent to the latency of the heterozygous littermates (Figure 4A) and was improved relative to untreated MPS IIIA mice. Additionally, MPS IIIA mice treated with AAV.SGSHv4 performed similar to their heterozygous littermates in spatial memory tests, assessed as the time spent and distance traveled in the target quadrant, while MPS IIIA mice treated with AAV.SGSH behaved similar to untreated disease mice (Figures 4B and 4C). Cumulatively, the data show that intraventricular injection of this dose of AAV.SGSHv4, but not AAV.SGSH, is sufficient to correct spatial learning and memory deficits in MPS IIIA mice.

SGSH activity in the CSF of AAV.SGSHv4-treated mice reached 80% of heterozygous levels, which was approximately twice that of AAV4.SGSH-treated mice (Figure 5A). To test the extent of diffusion, we dissected samples from the hippocampus, striatum, occipital cortex, and cerebellum and assessed enzyme activity. Untreated MPS IIIA tissues have ~1%–4% of heterozygous levels. MPS IIIA mice treated with AAV.SGSHv4 or AAV.SGSH had increased SGSH activity compared with untreated MPS IIIA mice; however, the activity in brain regions from AAV.SGSHv4-treated mice was approximately twice that of tissues from AAV.SGSH-treated mice. SGSH activity in AAV.SGSHv4-treated mice was 35%, 14.5%, 16%, and 14% of heterozygous levels in the hippocampus, striatum, occipital cortex, and cerebellum, respectively (Figure 5B).

We next evaluated the impact on characteristic storage and astrogliosis, using brain samples contralateral to or unilateral to the site of injection, respectively (Figures 6A and 6B). Treatment with AAV.SGSH or AAV.SGSHv4 reduced glycosaminoglycan (GAG) levels in all regions (Figure 6A), with SGSHv4 inducing a significantly greater reduction in hippocampal and striatal regions. Notably, there was no significant difference in GAG levels between AAV.SGSHv4-treated MPS IIIA mice and their heterozygous littermates in all examined regions. The impact of SGSHv4 treatment on the characteristic astrogliosis in MPS IIIA mice was striking and more robust than that seen in SGSH-treated animals (Figure 6B). Qualitatively, there was little observable difference between SGSHv4-treated MPS IIIA mice and heterozygous controls. Further studies to quantify glial fibrillary acidic protein (GFAP) immunoreactivity were done, and they demonstrated no differences between AAV.SGSHv4-treated animals and heterozygous controls in layers IV and V of the motor cortex, as well as the striatum (Figures 6C and 6D).

There is significant elevation of β-glu activity in MPS IIIA mice brain, which is secondary to SGSH deficiency.[17] β-Glu activity in the CSF of MPS IIIA mice was 160% of heterozygous levels, which decreased to 120% of heterozygous levels following AAV.SGSHv4 gene transfer, versus 147% of heterozygous levels after AAV.SGSH treatment (Figure 6E). In brain parenchyma, β-glu activities of MPS IIIA mice were significantly higher than those in heterozygous mice and were 185%, 242%, 237%, and 190% of heterozygous levels in hippocampus, striatum, occipital cortex, and cerebellum, respectively. AAV.SGSHv4 decreased β-glu activity levels to 120% and 166% of heterozygous levels in hippocampus and striatum, which is significantly lower than those found in tissue lysates from AAV.SGSH-treated mice (163% in hippocampus and 207% in striatum, relative to heterozygous levels). β-Glu activities in the occipital cortex and cerebellum of AAV.SGSHv4-treated MPS IIIA mice were decreased compared with untreated MPS IIIA mice and lower than AAV.SGSH-treated mice, but there was no statistically significant difference from each other (Figure 6F).

DISCUSSION

In our study, we found that SGSH had poor secretory properties that were significantly different from β-glu and TPP1, which were very

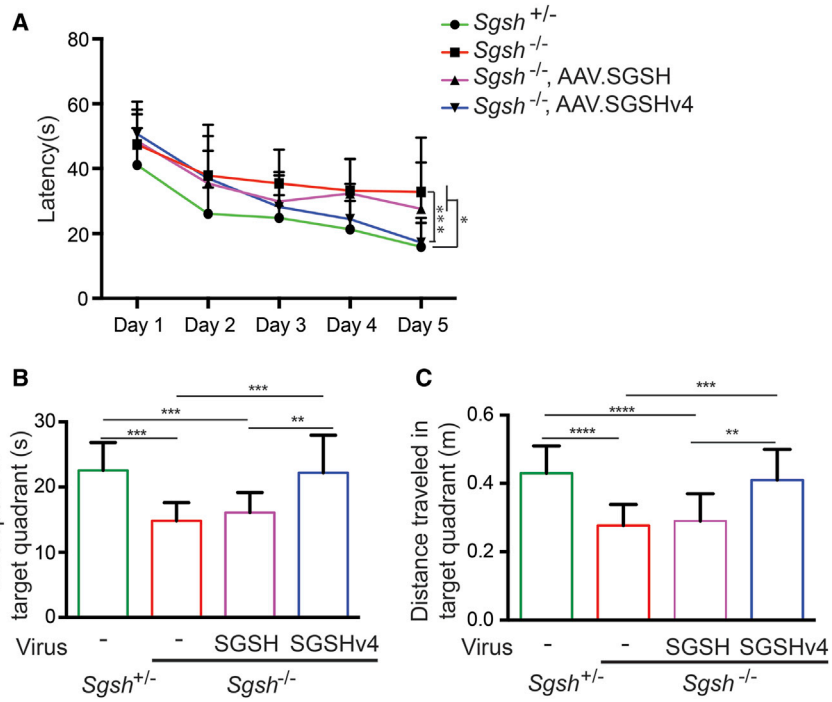

Figure 4. AAV.SGSHv4 Improves Behavioral Deficits in MPS IIIA Mice

Mice (8 wk old) were injected with AAV.SGSH or AAV.SGSH into lateral ventricle and animals tested in the Morris water maze 12 weeks later. (A) Latency to find the platform. (B) Time spent in the target quadrant on day 6. (C) Distance traveled in target quadrant on day 6. n = 14 for all groups. Data are mean ± SD. *p < 0.05; **p < 0.01; ***p < 0.001; ****p < 0.0001. One-way ANOVA followed by Tukey's post hoc test.

efficiently secreted. This mirrors very early studies in the cellular slime mold *Dictyostelium discoideum* and *Tetrahymena pyriformis*. In these model systems, under starvation conditions to minimize lysosomal enzyme synthesis, there were appreciable differences in secretory rates.[18,19] To improve SGSH secretion, we first tested if re-engineering the signal peptide (SP) to contain those from other highly secreted lysosomal enzymes, iduronate-2-sulphatase, β-glu, and TPP1, would be sufficient. There was a modest increase (~30%) when the SGSH SP was switched with the SPs from iduronate-2-sulphatase or TPP1. A similar strategy was tested by the Fraldi group,[20] whereby SGSH secretion was more robustly improved when replaced with the iduronate-2-sulphatase SP. The discrepancy between our studies may be explained by the use of different cells and assay conditions (MPS IIIA mouse embryonic fibroblast cells with 0.5% FBS versus HEK293 cells with 10% FBS in our work). Indeed, starvation induces lysosomal enzyme secretion.[21] In both studies, iduronate-2-sulphatase SP:SGSH chimera did not impact cellular SGSH levels, which remained higher in cells relative to the media. Because of the elevated SGSH load, we explored alternative methods for improving SGSH secretion.

Proper trafficking of SGSH requires posttranslational modification in the *trans*-Golgi apparatus (TGN), wherein enzyme association with the M6P receptor (M6PR) allows lysosome transport. For SGSH and many other lysosomal hydrolases, a proportion of the expressed protein can be secreted after entry into the secretory pathway. Secreted enzymes can bind the M6PR or mannose receptor on the plasma membrane of the same or different cells for entry and subsequent trafficking to the lysosome.[22] M6PR-deficient fibroblasts show significantly higher secretion of lysosomal hydrolases than normal cells.[23] In our earlier work, we found that generating a chimeric protein consisting of β-glu and the anionic TAT peptide reduced phosphorylation, improved secretion, and reduced uptake via M6PR.[24,25] The consequence of these alterations *in vivo* was improved biodistribution after gene transfer to brain.[24]

We screened all M6P binding sites in SGSH and found that modifying the fourth M6P binding site (SGSHv4) resulted in improved secretion and increased uptake that was M6PR independent, a finding similar to our work with the TAT-modified β-glu.[24,25] Further work is required to better understand their mechanism of uptake and whether it varies between different cell types.

In studies in MPS IIIA-deficient mice, transduction of the ependymal cells that line the ventricular surface with AAVs expressing SGSHv4 improved spatial learning, reduced memory deficits, reduced GAG levels and astrogliosis, and resolved secondary lysosomal enzyme elevations in the CSF and brain parenchyma. These data contrasted those obtained using AAVs expressing WT SGSH, where secretion into the CSF was significantly lower. There were reductions in GAG levels and astrogliosis with SGSH, but the impact was less robust and more notably, there were no significant improvements in behavior phenotypes. These data support earlier work showing that transduction of cells that can support secretion into the CSF, such as ependyma or the choroidal epithelium, both long-lived cells that rarely divide after birth, provides an excellent platform for the secretion of therapeutic proteins including soluble enzymes whose deficiencies affect the brain.[12,13,26]

We also tested if reducing SGSH degradation would be a useful strategy for improving SGSH secretion for gene therapy applications. Prior work from a proteome-wide *in vivo* ubiquitination study showed that SGSH has three ubiquitination sites.[15] We sequentially modified these three sites with no impact on secretory properties. Either modification exposes new sites for ubiquitination, or this approach will not be useful, at least for SGSH, for improving secretory properties.

In summary, we identified a variant SGSH with improved secretory and uptake properties that when delivered by AAV for transduction

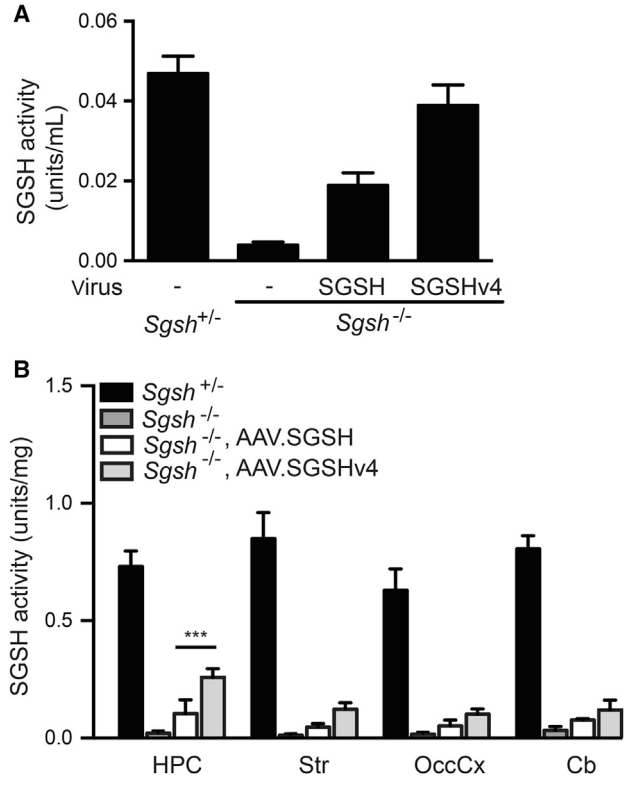

Figure 5. SGSH Activity in the CSF and Brain Tissue Lysates after rAAV.SGSH or rAAV.SGSHv4 Delivery

Mice (8 wk old) were injected with AAV.SGSH or AAV.SGSH into the lateral ventricle and CSF collected 14 weeks later, after which the mice were euthanized and tissues collected for SGSH activity assay. (A) SGSH activity in CSF pooled from four to six mice. (B) SGSH activity in brain parenchyma from the hippocampus (HPC), striatum (Str), occipital cortex (OccCx), and cerebellum (Cb). n = 6. Data represent mean ± SD. ***$p < 0.001$. One-way ANOVA followed by Tukey's post hoc test.

of ventricular lining cells showed greater *in vivo* benefit relative to the WT enzyme in a mouse model of MPS IIIA. A consequence of greater potency is that lower doses can be used for the same therapeutic benefit in human gene therapy applications for Sanfilippo A patients. This has the added advantage of improving safety profiles by reducing unwanted immune responses, which is important for lasting expression in humans.[27]

MATERIALS AND METHODS

SGSH Variant Construction

Human SGSH, TPP1, and β-glu genes were PCR amplified from a human cDNA library and cloned into the pFB.AAV.CMV.SV40pA backbone plasmid.[28] SGSH variants were constructed by overlap PCR with primer sets listed in Table S1.

Enzymes Assays

Lysosomal enzymes activity assay was measured using fluorogenic substrates. SGSH activity was measured by a two-step protocol[29] with 4-methylumbelliferone (Sigma) as standard. TPP1 activity was assayed as described previously,[12,30] with purified recombinant TPP1 standard provided from P. Lobel (State University of New Jersey). β-Glu activity was assayed as described previously[13] with 4-methylumbelliferone (4-MU) as standard. A unit is defined as the amount that will liberate 1 nmol 4-MU at 37°C from the respective fluorogenic substrate in 17 hr for SGSH or 1 hr for β-glu.

In Vitro Secretion Studies

Low-passage HEK293 cells were maintained in DMEM with 10% FBS. 24 hr before transfection, 4×10^4 cells were seeded into a 96-well plate in 100 μL of media. Transfections (100 ng of plasmid) were done using Lipofectamine 2000 (Invitrogen). After transfection (24, 48, or 72 hr based on different experiments), 100 μL of conditioned media was harvested for assay. Cell lysates were collected in 100 μL of normal saline with complete protease inhibitor cocktail (Roche) and 0.1% Triton X-100. Soluble lysosomal enzymes were released from cells by sonication for 2 s twice on ice. Insoluble material was removed by centrifugation at 21,000 × *g* for 15 min at 4°C.

Western Blots

Lysate or medium samples were loaded into 4%–12% SDS-PAGE gel and transferred to 0.45-μm polyvinylidene difluoride (PVDF) membrane. Primary mouse anti-SGSH 1:2,000 (gifted from Shire) and mouse anti-β-tubulin 1:2,000 (from Sigma) and secondary horseradish peroxidase (HRP)-labeled goat anti-mouse 1:20,000 (Cell Signaling Technology) were used. Blots were developed using ECL Plus Western Blotting Detection System (GE Healthcare) and exposed to film for images. Quantification was performed using the ChemiDoc Imaging System (Bio-Rad).

Cell Fractionation Studies

Subcellular fractions were enriched from HEK293 cell lysates collected 72 hr after transfection with SGSH- or SGSHv4-expression plasmids using a lysosome enrichment kit (Thermo Fisher) with modification. In brief, cells were collected from plates and centrifuged (600 × *g*, 5 min) and resuspended in hypotonic buffer (10 mM HEPES, 25 mM potassium chloride, 1 mM EGTA, 0.5 mM EDTA [pH 7.8]). After 5 min, samples were pelleted (600 × *g*, 5 min), resuspended, and Dounce homogenized (10 strokes) in isotonic buffer (10 mM HEPES, 250 mM sucrose, 25 mM potassium chloride, 1 mM EGTA, 0.5 mM EDTA [pH 7.8]). The homogenate was cleared of nuclei and debris (500 × *g*, 10 min) to obtain the post-nuclear fraction (PNF). The PNF was diluted to 15% with OptiPrep media and then layered onto a discontinuous OptiPrep gradient (17%, 20%, 23%, 27%, and 30%) and centrifuged (145,000 × *g*, 2 hr). After centrifugation, the distinct bands were collected, washed in PBS, recovered (18,000 × *g*, 30 min), and solubilized in lysis buffer (50 mM Tris [pH 8.0], 150 mM NaCl, 1% Nonidet P-40 [NP-40], 0.1% SDS, 0.5% deoxycholic acid, 1 mM beta-mercaptoethanol). After PAGE, proteins were transferred to nitrocellulose membranes and western blots were done using SGSH antibody (gift from Shire, 1:2,000), LAMP1 (Developmental Studies Hybridoma Bank [DSHB] at University of Iowa, 1:500), Rip/Grp78 (1:1,000; Cell Signaling Technology), and

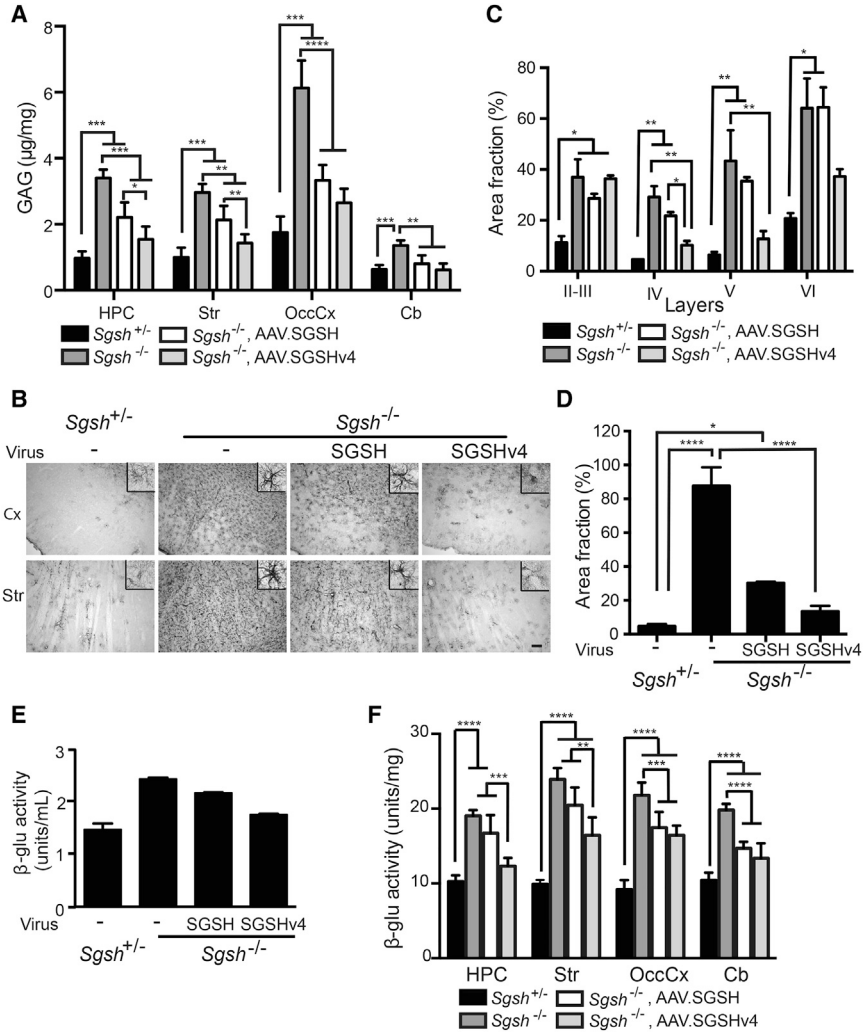

Figure 6. AAV.SGSHv4 Alleviates Neuropathology in MPS IIIA Mice

Mice (8 wk old) were injected with AAV.SGSH or AAV.SGSHv4 into the lateral ventricle. Animals were euthanized 14 weeks later, and tissues were harvested for analysis of impact on neuropathological readouts. (A) Quantification of GAG in parenchyma from tissues harvested contralateral to the injection site: hippocampus (HPC), striatum (Str), occipital cortex (OccCx), and cerebellum (Cb). n = 4–6. Data represent mean ± SD. *p < 0.05; **p < 0.01; ***p < 0.001; ****p < 0.0001. One-way ANOVA followed by Tukey's post hoc test. (B) Glial astrocytosis measured by immunoreactivity for GFAP in sections collected from hemispheres unilateral to the injection site. Representative photomicrographs are from the cortex (Cx) and striatum (Str); n = 3 mice per group, three sections/mouse. Scale bar, 100 μm. Insets show isolated GFAP-immunoreactive glia. (C and D) Threshold image analysis was used to measure the fraction of total area positive for GFAP immunoreactivity in the noted cortical layers (C) and striatum (D). Data represent mean ± SEM, three mice/group and three sections/mouse. For each section, analyses were done on three random fields (100 μm × 100 μm) in the indicated cortical layers and 12 random fields (100 μm × 100 μm) in the striatum. *p < 0.05; **p < 0.01; ****p < 0.0001, Kruskal-Wallis nonparametric test. (E and F) β-Glu activity in the CSF and brain tissue lysates after rAAV.SGSH or rAAV.SGSHv4 delivery. (E) β-Glu activity in CSF pooled from four to six mice. (F) β-Glu activity in brain parenchyma from indicated regions. n = 6. Data are mean ± SD. **p < 0.01; ***p < 0.001; ****p < 0.0001, one-way ANOVA followed by Tukey's post hoc test.

GRASP 65 (1:1,000; Santa Cruz Biotechnology). Blots were developed as above.

Enzyme Uptake

Human MPS IIIA fibroblast cells were maintained in DMEM with 10% FBS. 1.0×10^5 of cells were seeded into a 24-well plate. After 24 hr, media were changed to 300 μL of conditioned media (containing 100 nmol/mL SGSH activity derived from HEK293 cells transfected with plasmids expressing SGSH or SGSHv4) in the absence or presence of 10 mM M6P. After 6 hr, the conditioned media were removed and the cells were washed with 500 μL of Hank's balanced salt solution (HBSS) with Ca^{2+} and Mg^{2+} three times. The cells were harvested and processed for activity assay, western blot, or immunohistochemistry.

Immunofluorescence and Immunohistochemistry

Cells were washed with 500 μL of HBSS with Ca^{2+} and Mg^{2+} three times and fixed with 4% paraformaldehyde (PFA) in PBS for 10 min at room temperature and blocked and permeabilized (10% goat serum and 0.1% Triton X-100 in PBS) for 1 hr at room temperature. Cells were incubated with mouse anti-SGSH primary antibody (1:200) in PBS containing 2% goat serum overnight at 4°C, then Alexa-conjugated secondary antibody (Invitrogen) at 1:2,000 for 1 hr at room temperature. Cells were coverslipped with Fluoro-Gel mounting media (Electron Microscopy Sciences) and analyzed by fluorescent microscopy (Leica Microsystems).

For GFAP immunohistochemistry, animals were transcardially perfused with normal saline followed by 4% PFA. Brains were then extracted and post-fixed in 4% PFA for 24 hr and 40-μm-thick sections cut on a freezing microtome. The sections were incubated overnight with rabbit anti-GFAP antibody (1:2,000; Dako Cytomation). Secondary antibody was biotinylated goat anti-rabbit IgG (1:500; Jackson ImmunoResearch). Slides were developed with 3,3-diaminobenzidine (Sigma). Semi-quantification of GFAP-positive cells was performed by threshold image analysis as previously reported.[11] In brief, images were converted to 8-bit grayscale images via ImageJ software, and the thresholding function was used to set a black and white threshold. The "analyze particles" function was used

to sum up the total area of positive staining and calculate the fraction of the total positive area.

AAV Production

AAV4 vectors expressing human SGSH or SGSHv4 under control of the cytomegalovirus promoter were generated using standard triple transfection methods and purification by CsCl gradient centrifugation.[31] Titers were quantified by silver stain after gel electrophoresis (SDS-PAGE) and qPCR.

Animals, AAV Vector Administration, and Tissue Collection

All animal procedures were approved by the Children's Hospital of Philadelphia (CHOP) Institutional Animal Care and Use Committee (IACUC) committee. MPS IIIA mice[17,32] (B6.Cg-Sgsh^{mps3a}/PstJ from Jackson Laboratory) were purchased and maintained at CHOP. AAV4 vectors encoding SGSH or SGSHv4 enzyme were produced by the Research Vector Core at CHOP by triple transfection in HEK293 cells and CsCl purification. Eight-week-old MPS IIIA mice ($Sgsh^{-/-}$) or heterozygous ($Sgsh^{+/-}$) mice of mixed gender were anesthetized with isoflurane. AAV vectors (5×10^{10} gp) were injected into the lateral ventricles (anteroposterior [A/P] −2.18 mm, mediolateral [M/L] −2.9 mm, dorsoventral [D/V] −3.5 mm) in 10 μL at 0.3 μL/min after mounting the mice on the stereotactic rig. The mice were euthanized at 22 weeks of age after behavioral testing was complete. CSF was collected by glass capillary inserted into the cisterna magna under a dissecting microscope. After CSF collection, mice were perfused with cold PBS, and brain regions were harvested. Brain tissues were homogenized in 200 μL of ice-cold homogenization buffer (0.1% Triton X-100 in normal saline with complete protease inhibitor cocktail; Roche) for enzyme assays.

Morris Water Maze

Morris water maze was performed 12 weeks after injection essentially as described.[33] In brief, a 100-cm-diameter pool was filled three-fourths full of water clouded with titanium (IV) oxide (Sigma). The pool was arbitrarily divided into quadrants. A transparent platform was placed 0.5 cm below the surface of the water in one quadrant (named target quadrant). Mice went through 5 days of acquisition with four trials each day. In each trial, the mice were released into the water facing a pre-defined direction. They had 60 s to locate the platform and were allowed 15 s on the platform. If this was not achieved, they were guided to platform. In each trial, the latency to find the platform was recorded. Probe trial was performed on day 6. The platform was removed and the start position was in the quadrant opposite the target quadrant. Time spent and distance traveled in the target quadrant were recorded (maximum time 60 s). Data were analyzed by Any-maze behavioral tracking software (ANY-maze).

GAG Assay

Brain tissues from the contralateral injected side were weighted and digested with Proteinase K. GAG levels were quantified with a glycosaminoglycan kit (Chondrex) using chondroitin 4-sulfate as standard. Results were normalized to wet tissue weight.

SUPPLEMENTAL INFORMATION

Supplemental Information includes two figures and one table and can be found with this article online at https://doi.org/10.1016/j.ymthe.2018.01.010.

AUTHOR CONTRIBUTIONS

Y.C. designed and performed experiments, interpreted the data, and wrote the manuscript. S.Z. and L.T. performed experiments. B.L.D. designed experiments, interpreted the data, and wrote the manuscript.

CONFLICTS OF INTEREST

B.L.D. is a founder of Spark Therapeutics, Inc. and is on the SAB of Intellia Therapeutics and Sarepta Therapeutics. This work was not sponsored by nor the findings licensed to these entities at the time of this work.

ACKNOWLEDGMENTS

We thank lab members Matt Sowada for mouse colony management and Elena Lysenko for mouse sample collection, and the Research Vector Core at the Children's Hospital of Philadelphia for AAV vector preparation. This work was funded by the National MPS Society and the Children's Hospital of Philadelphia Research Institute.

REFERENCES

1. Muenzer, J. (2004). The mucopolysaccharidoses: a heterogeneous group of disorders with variable pediatric presentations. J. Pediatr. *144* (*Suppl 1*), S27–S34.
2. Gliddon, B.L., and Hopwood, J.J. (2004). Enzyme-replacement therapy from birth delays the development of behavior and learning problems in mucopolysaccharidosis type IIIA mice. Pediatr. Res. *56*, 65–72.
3. Hemsley, K.M., King, B., and Hopwood, J.J. (2007). Injection of recombinant human sulfamidase into the CSF via the cerebellomedullary cistern in MPS IIIA mice. Mol. Genet. Metab. *90*, 313–328.
4. Marshall, N.R., Hassiotis, S., King, B., Rozaklis, T., Trim, P.J., Duplock, S.K., Winner, L.K., Beard, H., Snel, M.F., Jolly, R.D., et al. (2015). Delivery of therapeutic protein for prevention of neurodegenerative changes: comparison of different CSF-delivery methods. Exp. Neurol. *263*, 79–90.
5. Haurigot, V., Marcó, S., Ribera, A., Garcia, M., Ruzo, A., Villacampa, P., Ayuso, E., Añor, S., Andaluz, A., Pineda, M., et al. (2013). Whole body correction of mucopolysaccharidosis IIIA by intracerebrospinal fluid gene therapy. J. Clin. Invest. *123*, 3254–3271.
6. Ruzo, A., Marcó, S., García, M., Villacampa, P., Ribera, A., Ayuso, E., Maggioni, L., Mingozzi, F., Haurigot, V., and Bosch, F. (2012). Correction of pathological accumulation of glycosaminoglycans in central nervous system and peripheral tissues of MPSIIIA mice through systemic AAV9 gene transfer. Hum. Gene Ther. *23*, 1237–1246.
7. Fu, H., Cataldi, M.P., Ware, T.A., Zaraspe, K., Meadows, A.S., Murrey, D.A., and McCarty, D.M. (2016). Functional correction of neurological and somatic disorders at later stages of disease in MPS IIIA mice by systemic scAAV9-hSGSH gene delivery. Mol. Ther. Methods Clin. Dev. *3*, 16036.
8. Tardieu, M., Zérah, M., Husson, B., de Bournonville, S., Deiva, K., Adamsbaum, C., Vincent, F., Hocquemiller, M., Broissand, C., Furlan, V., et al. (2014). Intracerebral administration of adeno-associated viral vector serotype rh.10 carrying human SGSH and SUMF1 cDNAs in children with mucopolysaccharidosis type IIIA disease: results of a phase I/II trial. Hum. Gene Ther. *25*, 506–516.
9. Gilkes, J.A., Bloom, M.D., and Heldermon, C.D. (2016). Mucopolysaccharidosis IIIB confers enhanced neonatal intracranial transduction by AAV8 but not by 5, 9 or rh10. Gene Ther. *23*, 263–271.

10. Chen, Y.H., Claflin, K., Geoghegan, J.C., and Davidson, B.L. (2012). Sialic acid deposition impairs the utility of AAV9, but not peptide-modified AAVs for brain gene therapy in a mouse model of lysosomal storage disease. Mol. Ther. *20*, 1393–1399.

11. Chang, M., Cooper, J.D., Sleat, D.E., Cheng, S.H., Dodge, J.C., Passini, M.A., Lobel, P., and Davidson, B.L. (2008). Intraventricular enzyme replacement improves disease phenotypes in a mouse model of late infantile neuronal ceroid lipofuscinosis. Mol. Ther. *16*, 649–656.

12. Katz, M.L., Tecedor, L., Chen, Y., Williamson, B.G., Lysenko, E., Wininger, F.A., Young, W.M., Johnson, G.C., Whiting, R.E., Coates, J.R., and Davidson, B.L. (2015). AAV gene transfer delays disease onset in a TPP1-deficient canine model of the late infantile form of Batten disease. Sci. Transl. Med. *7*, 313ra180.

13. Liu, G., Martins, I., Wemmie, J.A., Chiorini, J.A., and Davidson, B.L. (2005). Functional correction of CNS phenotypes in a lysosomal storage disease model using adeno-associated virus type 4 vectors. J. Neurosci. *25*, 9321–9327.

14. Chang, M., Cooper, J.D., Davidson, B.L., van Diggelen, O.P., Elleder, M., Goebel, H.H., Golabek, A.A., Kida, E., Kohlschutter, A., Lobel, P., et al. (2011). CLN2. In The Neuronal Ceroid Lipofuscinoses (Batten Disease), S.E. Mole, R. Williams, and H.H. Goebel, eds. (Oxford University Press), pp. 80–109.

15. Wagner, S.A., Beli, P., Weinert, B.T., Nielsen, M.L., Cox, J., Mann, M., and Choudhary, C. (2011). A proteome-wide, quantitative survey of in vivo ubiquitylation sites reveals widespread regulatory roles. Mol. Cell Proteomics *10*, M111.013284.

16. Davidson, B.L., Stein, C.S., Heth, J.A., Martins, I., Kotin, R.M., Derksen, T.A., Zabner, J., Ghodsi, A., and Chiorini, J.A. (2000). Recombinant adeno-associated virus type 2, 4, and 5 vectors: transduction of variant cell types and regions in the mammalian central nervous system. Proc. Natl. Acad. Sci. USA *97*, 3428–3432.

17. Bhaumik, M., Muller, V.J., Rozaklis, T., Johnson, L., Dobrenis, K., Bhattacharyya, R., Wurzelmann, S., Finamore, P., Hopwood, J.J., Walkley, S.U., and Stanley, P. (1999). A mouse model for mucopolysaccharidosis type III A (Sanfilippo syndrome). Glycobiology *9*, 1389–1396.

18. Dimond, R.L., Burns, R.A., and Jordan, K.B. (1981). Secretion of lysosomal enzymes in the cellular slime mold, Dictyostelium discoideum. J. Biol. Chem. *256*, 6565–6572.

19. Banno, Y., Sasaki, N., and Nozawa, Y. (1987). Secretion heterogeneity of lysosomal enzymes in Tetrahymena pyriformis. Exp. Cell Res. *170*, 259–268.

20. Sorrentino, N.C., D'Orsi, L., Sambri, I., Nusco, E., Monaco, C., Spampanato, C., Polishchuk, E., Saccone, P., De Leonibus, E., Ballabio, A., and Fraldi, A. (2013). A highly secreted sulphamidase engineered to cross the blood-brain barrier corrects brain lesions of mice with mucopolysaccharidoses type IIIA. EMBO Mol. Med. *5*, 675–690.

21. Holtzman, E. (1989). Extensive release. Excessive storage. In Lysosomes (Springer), pp. 319–361.

22. Griffey, M.A., Wozniak, D., Wong, M., Bible, E., Johnson, K., Rothman, S.M., Wentz, A.E., Cooper, J.D., and Sands, M.S. (2006). CNS-directed AAV2-mediated gene therapy ameliorates functional deficits in a murine model of infantile neuronal ceroid lipofuscinosis. Mol. Ther. *13*, 538–547.

23. Ludwig, T., Munier-Lehmann, H., Bauer, U., Hollinshead, M., Ovitt, C., Lobel, P., and Hoflack, B. (1994). Differential sorting of lysosomal enzymes in mannose 6-phosphate receptor-deficient fibroblasts. EMBO J. *13*, 3430–3437.

24. Xia, H., Mao, Q., and Davidson, B.L. (2001). The HIV Tat protein transduction domain improves the biodistribution of beta-glucuronidase expressed from recombinant viral vectors. Nat. Biotechnol. *19*, 640–644.

25. Orii, K.O., Grubb, J.H., Vogler, C., Levy, B., Tan, Y., Markova, K., Davidson, B.L., Mao, Q., Orii, T., Kondo, N., and Sly, W.S. (2005). Defining the pathway for Tat-mediated delivery of beta-glucuronidase in cultured cells and MPS VII mice. Mol. Ther. *12*, 345–352.

26. Hudry, E., Dashkoff, J., Roe, A.D., Takeda, S., Koffie, R.M., Hashimoto, T., Scheel, M., Spires-Jones, T., Arbel-Ornath, M., Betensky, R., et al. (2013). Gene transfer of human Apoe isoforms results in differential modulation of amyloid deposition and neurotoxicity in mouse brain. Sci. Transl. Med. *5*, 212ra161.

27. Ertl, H.C.J., and High, K.A. (2017). Impact of AAV capsid-specific T-cell responses on design and outcome of clinical gene transfer trials with recombinant adeno-associated viral vectors: an evolving controversy. Hum. Gene Ther. *28*, 328–337.

28. Urabe, M., Ding, C., and Kotin, R.M. (2002). Insect cells as a factory to produce adeno-associated virus type 2 vectors. Hum. Gene Ther. *13*, 1935–1943.

29. Karpova, E.A., Voznyi, Y.a.V., Keulemans, J.L., Hoogeveen, A.T., Winchester, B., Tsvetkova, I.V., and van Diggelen, O.P. (1996). A fluorimetric enzyme assay for the diagnosis of Sanfilippo disease type A (MPS IIIA). J. Inherit. Metab. Dis. *19*, 278–285.

30. Tian, Y., Sohar, I., Taylor, J.W., and Lobel, P. (2006). Determination of the substrate specificity of tripeptidyl-peptidase I using combinatorial peptide libraries and development of improved fluorogenic substrates. J. Biol. Chem. *281*, 6559–6572.

31. Ayuso, E., Mingozzi, F., Montane, J., Leon, X., Anguela, X.M., Haurigot, V., Edmonson, S.A., Africa, L., Zhou, S., High, K.A., et al. (2010). High AAV vector purity results in serotype- and tissue-independent enhancement of transduction efficiency. Gene Ther. *17*, 503–510.

32. Bhattacharyya, R., Gliddon, B., Beccari, T., Hopwood, J.J., and Stanley, P. (2001). A novel missense mutation in lysosomal sulfamidase is the basis of MPS III A in a spontaneous mouse mutant. Glycobiology *11*, 99–103.

33. Vorhees, C.V., and Williams, M.T. (2006). Morris water maze: procedures for assessing spatial and related forms of learning and memory. Nat. Protoc. *1*, 848–858.

YMTHE, Volume *26*

Supplemental Information

Overcoming Limitations Inherent in Sulfamidase to Improve Mucopolysaccharidosis IIIA Gene Therapy

Yonghong Chen, Shujuan Zheng, Luis Tecedor, and Beverly L. Davidson

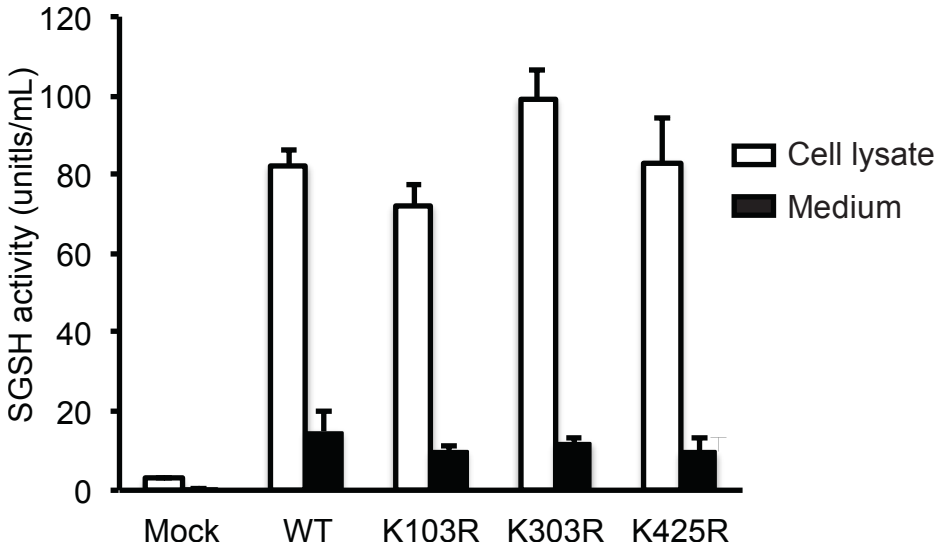

Fig. S1. Effects of ubiquitination site modifications on SGSH enzyme secretion. Three SGSH variants were generated by mutagenesis (K-to-R) to eliminate known ubiquitin binding sites at K103, K303 and K425 (Table S1). Vectors expressing wild type or SGSH variants were transfected into HEK 293 cells and cells and media collected and assayed for SGSH enzyme activity, n=3, data are mean ± SD.

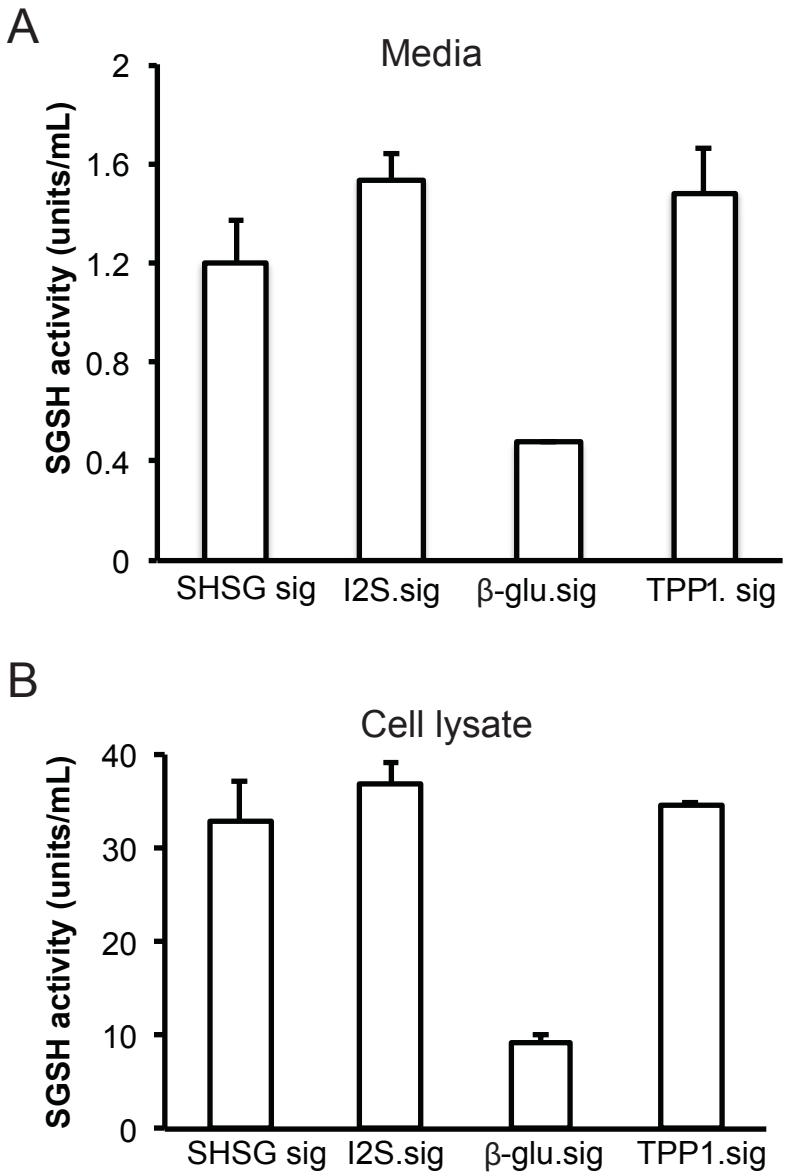

Fig. S2. Effects of different signal peptides on SGSH enzyme secretion. SGSH signal peptide was substituted with signal peptides from iduronate-2-sulphatase (I2S), β-Glu or TPP1. Vectors were transfected into HEK 293 cells and media (a) and cells (b) collected and assayed for SGSH enzyme activity, n=3, data are mean ± SD.

Table S1. Primer sequences for the construction of the SGSH variants

M6P variants	Mutation site	Primer	
SGSHv1	N41Q	Primer 1	CTCGAGGCCACCATGAGCT
		Primer 2	CGATGGCGCTGTTCTGGTACG
		Primer 3	GCGTACCAGAACAGCGCCATC
		Primer 4	GACGGAGGTCCTTGTACCAG
SGSHv2	N142Q	Primer 1	CTCGAGGCCACCATGAGCT
		Primer 2	GACGGAGCCCTGCTCCTCC
		Primer 3	GGAGGAGCAGGGCTCCGTC
		Primer 4	GACGGAGGTCCTTGTACCAG
SGSHv3	N151Q	Primer 1	CTCGAGGCCACCATGAGCT
		Primer 2	GCTTAATTCTAGTGATCTGCCGCC
		Primer 3	GGCGGCAGATCACTAGAATTAAGC
		Primer 4	GACGGAGGTCCTTGTACCAG
SGSHv4	N264Q	Primer 1	CTCGAGGCCACCATGAGCT
		Primer 2	CCAGTGTGTCCTGCAGGACAC
		Primer 3	GTGTCCTGCAGGACACACTGG
		Primer 4	GACGGAGGTCCTTGTACCAG
SGSHv5	N413Q	Primer 1	CTCGAGGCCACCATGAGCT
		Primer 2	GTGGTGCGCTGCAGGAGGTC
		Primer 3	GACCTCCTGCAGCGCACCAC
		Primer 4	GACGGAGGTCCTTGTACCAG
Ubiquitin variants			
SGSH.Uv1	K103R	Primer 1	CTCGAGGCCACCATGAGCT
		Primer 2	GCTCCGCACCCGGTCGAAGG
		Primer 3	CCTTCGACCGGGTGCGGAGC
		Primer 4	GACGGAGGTCCTTGTACCAG
SGSH.Uv2	K303R	Primer 1	CTCGAGGCCACCATGAGCT
		Primer 2	CCCAGCGGCGTGGGTGCTC
		Primer 3	CCCAGCGGCGTGGGTGCTC
		Primer 4	GACGGAGGTCCTTGTACCAG
SGSH.Uv3	K425R	Primer 1	CTCGAGGCCACCATGAGCT
		Primer 2	GACGGAGGTCCCGGTACCAGC